AD-A187 562 ATOMIC AND MOLECULAR GAS PHASE SPECTROMETRY(U) FLORIDA 1/1
UNIV GAINESVILLE DEPT OF CHEMISTRY J D WINEFORDNER
1987 AFOSR-TR-87-1581 AFOSR-86-0015

UNCLASSIFIED F/G 7/2 NL

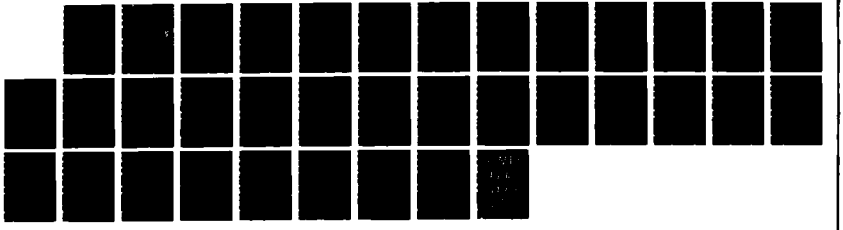

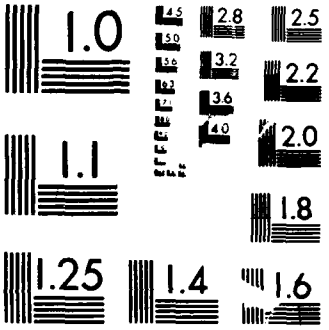

MICROCOPY RESOLUTION TEST CHART
NATIONAL BUREAU OF STANDARDS 1963-A

DTIC FILE COPY

UNCLASSIFIED
SECURITY CLASSIFICATION OF THIS PAGE

2

REPORT DOCUMENTATION PAGE

Form Approved
OMB No. 0704-0188

1a. REPORT SECURITY CLASSIFICATION UNCLASSIFIED	1b. RESTRICTIVE MARKINGS
AD-A187 562	3. DISTRIBUTION/AVAILABILITY OF REPORT Approved for public release; Distribution unlimited
	5. MONITORING ORGANIZATION REPORT NUMBER(S) AFOSR-TR- 87-1581

6a. NAME OF PERFORMING ORGANIZATION Department of Chemistry University of Florida	6b. OFFICE SYMBOL *(If applicable)*	7a. NAME OF MONITORING ORGANIZATION AFOSR/NC
6c. ADDRESS *(City, State, and ZIP Code)* University of Florida Gainesville, FL 32611		7b. ADDRESS *(City, State, and ZIP Code)* Bldg 410 Bolling AFB DC 20332-6448
8a. NAME OF FUNDING/SPONSORING ORGANIZATION AFOSR	8b. OFFICE SYMBOL *(If applicable)* NC	9. PROCUREMENT INSTRUMENT IDENTIFICATION NUMBER AFOSR-86-0015
8c. ADDRESS *(City, State, and ZIP Code)* Bldg 410 Bolling AFB DC 20332-6448		10. SOURCE OF FUNDING NUMBERS

PROGRAM ELEMENT NO.	PROJECT NO.	TASK NO	WORK UNIT ACCESSION NO
61102F	2303	A1	

DTIC ELECTE NOV 12 1987 S E

11. TITLE *(Include Security Classification)*
"Atomic and Molecular Gas Phase Spectrometry"

12. PERSONAL AUTHOR(S)

13a. TYPE OF REPORT	13b. TIME COVERED	14. DATE OF REPORT *(Year, Month, Day)*	15. PAGE COUNT
FINAL	FROM 10ct85 TO 30Sep87		32

16. SUPPLEMENTARY NOTATION

17. COSATI CODES			18. SUBJECT TERMS *(Continue on reverse if necessary and identify by block number)*
FIELD	GROUP	SUB-GROUP	Atomic spectroscopy, analytical chemistry, gases

19. ABSTRACT *(Continue on reverse if necessary and identify by block number)*

The research involves an extensive investigation of analytical and physical aspects of gas phase spectroscopy. The goal of these studies is the development of high sensitivity, high selectivity, precise, accurate methods of analysis of elements in real samples by atomic adsorption, atomic emission, atomic fluorescence, atomic ionization, and atomic photothermal methods. The major research projects have included: evaluation of the mechanism of vaporization, atomization, excitation, and ionization of N2 molecules in the ICP; derivation of expressions to describe analytical growth curves in AFS; measurement of OH rotational population distributions in combustion flames and evaluation of the departures from thermal equilibrium; evaluation of the analytical uses of flame and furnace coherent forward scatter spectrometry using both lasers and continuum conventional sources; evaluation of a Cu-vapor pumped dye laser and several detection methods for atomic fluorescence and atomic ionization; evaluation of laser

20 DISTRIBUTION/AVAILABILITY OF ABSTRACT	21. ABSTRACT SECURITY CLASSIFICATION
☒ UNCLASSIFIED/UNLIMITED ☒ SAME AS RPT. ☐ DTIC USERS	Unclassified (over)

22a. NAME OF RESPONSIBLE INDIVIDUAL	22b. TELEPHONE *(Include Area Code)*	22c. OFFICE SYMBOL
Dr John Wilkes	(303)472-2655	NC

DD Form 1473, JUN 86 *Previous editions are obsolete.* SECURITY CLASSIFICATION OF THIS PAGE

excitation of atoms in graphite furnaces and ICPs as analytical methods; diagnostical studies of the effect of RF power, cooling gas flow rate and height on atomic fluorescence and emission measurements using the extended torch ICP; development and evaluation of surface burners to produce diffusion flames for atomic spectrometry; and evaluation of analytical and diagnostical methods for flames based upon laser excitation and polarization, photothermal, and saturated interference measurements.

FINAL TECHNICAL REPORT AFOSR-86-0015

TITLE: Atomic and Molecular Gas Phase Spectrometry

PRINCIPAL INVESTIGATOR: J.D. Winefordner

ADDRESS: Department of Chemistry
University of Florida
Gainesville, FL 32611

PROGRAM MANAGER: John Wilkes

AFOSR-TR- 87-1581

REPORT PERIOD: Oct. 1, 1985 - Sept. 30, 1987

RESEARCH STAFF:

J.D. Winefordner	Principal Investigator
Ben Smith	Research Associate
B. Patel	Post Doctoral Research Associate
T. Hasegawa	Post Doctoral Research Associate
K.P. Li	Post Doctoral Research Associate
Mahmood Chamsaz	Post Doctoral Research Associate
Jim Deavor	Post Doctoral Research Associate
Lori Davis	Graduate Research Assistant
Doug Goforth	Graduate Research Assistant
Jose Lanauze	Graduate Research Assistant
Mario Tremblay	Graduate Research Assistant
Tom Manning	Graduate Research Assistant
Paul Johnson	Graduate Research Assistant
Wellington Masamba	Graduate Research Assistant
Jorge Vera	Graduate Research Assistant
Moi Leong	Graduate Research Assistant
Joe Simeonsson	Graduate Research Assistant
Chris Stevenson	Graduate Research Assistant
Abdalla Ali	Graduate Research Assistant
Ben Womack	Graduate Research Assistant

Accession For
NTIS GRA&I [X]
DTIC TAB [ ]
Unannounced [ ]
Justification
By
Distribution/
Availability Codes
Dist | Avail and/or Special
A-1

DTIC COPY INSPECTED 1

87 10 22 036

ABSTRACT

The research involves an extensive investigation of analytical and physical aspects of gas phase spectroscopy. The goal of these studies is the development of high sensitivity, high selectivity, precise, accurate methods of analysis of elements in real samples by atomic absorption, atomic emission, atomic fluorescence, atomic ionization, and atomic photothermal methods. The major research projects have included: evaluation of the mechanism of vaporization, atomization, excitation, and ionization of N_2 molecules in the ICP; derivation of expressions to describe analytical growth curves in AFS; measurement of OH rotational population distributions in combustion flames and evaluation of the departures from thermal equilibrium; evaluation of the analytical uses of flame and furnace coherent foward scatter spectrometry using both lasers and continuum conventional sources; evaluation of a Cu-vapor pumped dye laser and several detection methods for atomic fluorescence and atomic ionization; evaluation of laser excitation of atoms in graphite furnaces and ICPs as analytical methods; diagnostical studies of the effect of RF power, cooling gas flow rate and height on atomic fluorescence and emission measurements using the extended torch ICP; development and evaluation of surface burners to produce diffusion flames for atomic spectrometry; and evaluation of analytical and diagnostical methods for flames based upon laser excitation and polarization, photothermal, and saturated interference measurements.

PROGRESS REPORT

Review of Methods. The use of the inductively coupled plasma, ICP, as a source and as a cell in atomic fluorescence spectrometry, AFS, is reviewed by Omenetto and Winefordner (1). These workers give the major references concerning the ICP in analytical AFS and discuss the use of the ICP as a source for atoms in flames, furnaces, and plasmas and the use of the ICP as a cell with conventional as well as laser source excitation. The same authors (2) review scattering in AFS. In the latter review, scattering is defined and expressions are given for the intensity of scatter from gaseous species as well as particulates. Seventeen methods of correcting for scatter errors in AFS are discussed in detail. The correction methods include: non-resonance fluorescence, wavelength scanning, wavelength modulation, two line method with one or two sources, quenching based method, polarization based method, source profile method, time resolution method, Zeeman method, intermodulation and harmonic saturated methods, double resonance and 2-photon methods, sensitized fluorescence, wing excitation method, and photodissociation-photoionization based methods.

Fundamental Studies. The mechanisms of excitation of atoms and ions in the ICP have been further studied by Hasegawa and Winefordner (3-5). In the first paper (3), number densities of atomic and molecular species in the ICP were estimated in the following way. Based on the Collisional-Radiative (CR) model, calculations of electronic level number densities of the hydrogen atom and the nitrogen molecule, their ground state densities were determined from T_e (electron temperature), T_g (gas temperature), n_e (electron density) and absolute emission intensities. For other species, thermal equilibrium described by T_g was assumed, considering the reaction rates for dissociation processes.

The calculated spatial profiles showed that an aqueous solution is efficiently introduced into the narrow central channel and is almost completely decomposed to hydrogen and oxygen atoms and diffused in the lateral direction with increasing height. Contrary to hydrogen and oxygen, nitrogen was preferentially present as N_2 molecules because of its relatively high dissociation energy. The N_2 profiles also indicated the off-axis high temperature zone at lower plasma heights minimized air entrainment from surrounding atmosphere, but the concentration of N_2 and O_2 rapidly increased up to about $1x10^{18}$ cm^{-3} at a height of 65 mm due to the bell shape configuration of temperature.

Diagnostics of nitrogen molecules in the ICP have been evaluated with respect to collisional processes with electrons, argon atoms and nitrogen molecules (4). Based on reaction probabilities, defined as the product of the rate coefficient and number density of colliding species, argon collisions were proposed as the dominant excitation mechanism for rotational transitions of N_2, while vibrational transitions showed complex behavior depending upon the vibrational quantum number. Furthermore, the excitation mechanism for electronic levels was considered by applying the collisional-radiative (CR) model including heavy particle collisions, such as mutual N_2 impact and Penning processes.

The present excitation model for nitrogen molecules in the ICP has led to the following conclusions.

(i) Rotational transitions are dominated by argon atom collisions. As a result, N_2-T_{rot} is considered to be close to T_g of Ar.

(ii) Vibrational temperature, T_{vib}, is predominately caused by electron impact for lower vibrational levels, while higher vibrational levels are subject to argon collisions.

(iii) Electron collisions, are, as a whole, the main processes for electronic excitation and de-excitation. However, spontaneous emission largely contributes to the B-C transition, which results in the underpopulation of the C state compared to the LTE value.

Temperature measurements for neutral nitrogen molecules in the ICP were obtained from the emission spectra of the N_2 second positive bands by using a medium resolution monochromator (5). The rotational temperature, T_{rot} estimated from the half-widths of the over-all band profile, was approximately 4000 K around the observation height of 70 mm, which was substantially higher than that of OH (2000 K). T_{vib} was in the range of 2500-5500 K and had a similar spatial profile as those of T_{exc} or T_e reported previously, namely an annular structure which changes to a bell-shape with increasing observation height. Detailed considerations on the energy balance in the plasma suggested that the energies gained by nitrogen molecules through collisions with electrons were lost by heat conduction in the radial direction, and collisions between N_2 and Ar were thermally equilibrated. The N_2 band emission intensities and vibrational temperatures showed the significance of air entrainment from the surrounding atmosphere at higher positions in the ICP.

Spatial distributions of Na resonance level lifetimes in the inductively coupled plasma (ICP) were measured by time-resolved laser-excited fluorimetry. In order to elucidate the quenching mechanism, the lifetimes obtained were

compared to theoretical values estimated from the quenching rate coefficients and number densities of colliding species. As a result, it was shown that resonance level Na atoms were mainly deactivated by electrons at lower heights in the plasma, while collisions with nitrogen molecules entrained from the surrounding atmosphere dominated the quenching reaction in the tail flame region.

Zizak, et al. (6) measured the rotational population distribution of OH in three different flames by laser-excited fluorescence. We have confirmed the results of Crosley for the methane-air flame and extended the analysis to a methane-oxygen-argon and acetylene-air flames. The distributions appeared to be strongly dependent on the laser excited level and only minor effects seem to be related to the gas composition and temperature. When exciting low levels (1-5), the slope of the distribution for the higher levels (10-15), appeared to be temperature and composition sensitive. Thus, accurate temperature measurements were possible only in very specific cases or if previous knowledge of the individual branching ratio, R_{ic}/Q_i for the higher levels is available.

Smith, et al. (7) have shown how to estimate absolute number densities (cm^{-3}) from the shapes of atomic fluorescence growth curves. From the expression given and the measurements made, it was apparent that with increasing number density, the point of departure from linearity did not depend very strongly on the parameters which affect the curve shape but was related to the oscillator strength of the atomic transition and the pathlength over which fluorescence is produced. It was therefore possible to obtain an approximate absolute atomic number density in a plasma or flame by measuring a complete fluorescence COG and noting the point at which the upper end departs from linearity. Referring to Table 1, this point occurred at values of k_oL ranging

from 0.7 to 6.0, depending upon the relative halfwidths of the excitation and absorption profiles and the damping parameter. Prefiltering shifted the point of departure from linearity much more so than post-filtering, and the combined effects caused departure from linearity at number densities an order of magnitude or more lower than when no filtering effects were present. Our treatment applied for linear interaction between the absorbing atoms and the radiation and so if useful when non-laser sources were used. However, it was easy to realize that the same treatment was also applicable for saturated conditions with laser excitation. In this case, if the laser was able to bleach the transition also at high atomic densities, only post-filter effects would need to be considered. On the other hand, saturation broadening and other effects would also complicate the treatment; work is underway to provide a similar treatment as the present one to the shape of laser excited fluorescence and ionization growth curves.

TABLE 1

Variation of the $(k_oL)_{3dB}$ Values with Different Values of the Damping Parameter and Source Profile to Absorbing Doppler Width Ratio

$\Delta\lambda_s/\Delta\lambda_D$	0.01	0.1	1.0	2.0
0.05	0.68	0.78	1.8	3.1
0.5	0.72	0,81	1.9	3.2
1	0.76	0.86	2.0	3.3
5	0.81	0.93	2.4	3.9
10	1.0	1.1	2.5	4.1
50	1.1	1.2	2.7	4.6
500	1.1	1.2	2.8	5.6

Expressions (8) have been given for emission, absorption and fluorescence with line and continuum source excitation which allow determination of the absolute number density of species present in a flame or plasma. The calculated results from these expressions and the experimentally determined results showed that the intersection point of the low and high concentration asymptopes were within one order of magnitude for all three methods. In contrast to many methods for determination of number densities, absolute calibration of the source or the detector was not required and a minimal knowledge of the atom and source characteristics was needed. Absolute elemental analysis (within a factor of 2-3X) is certainly a possibility.

Coherent Forward Scatter Spectrometry (CFSS). Davis and Winefordner (9-11) have evaluated Coherent Forward Scatter Spectrometry (CFSS), as an analytical method. Coherent forward scattering atomic spectrometry involves the rotation of polarized light by atoms located within a transverse or a longitudinal magnetic field, the Voigt and Faraday effect, respectively. Davis and Winefordner (8) used a continuum source to excite simultaneously all atomic transitions. A set of polarizers was used before and after the atom reservoir to polarize initially the incident light and detect the rotated light, respectively. This study employed both an air-acetylene flame and a graphite furnace as atom reservoirs. A DC transverse magnetic field was employed around the atom reservoir. A monochromator, a photomultiplier and a lock-in amplifier form the detection system. The analytical figures of merit for several elements using the system were determined. While the limits of detection (LODs) for the flame were poor, the absolute LODs for the graphite furnace showed some promise in view of the multi-element capabilities of CFS in analytical chemistry (see Table 2).

The LODs of the present system (see Table 2) should be greatly improved by using a more intense continuum source which has better optical qualities; this should lead to an improved signal-to-noise ratio. It would be advantageous to increase the source intensity to the point that the blank (the light passing through the crossed polarizers) was increased sufficiently to be the same order of magnitude as the flame emission or the dark current of the PM tube. The LOD for Pb at 283.306 nm could be decreased by use of quartz polarizers, which would also allow evaluation of Zn and As at 213.856 nm and 197.2 nm, respectively.

TABLE 2

Limits of Detection (S/N = 3) for Multi-Element CFS

Element	Wavelength	Flame (µg/mL)	Furance (ng)[a]
Ca	422.673	0.1 (0.7)[b]	--
Cr	357.869	3 (6)[b]	--
Cu	324.754	0.2	0.3 (0.5)[b]
Pb	283.306	3	3
Mg	285.213	0.05 (0.2)[b]	--
Mn	279.482	- (1)[b]	--
Ag	328.068	0.3 (3)[b]	0.1
Na	588.995	0.04	0.04
Sr	460.733	0.6	0.2
Tl	377.572	2	--

While the LODs for the continuum source CFS system are poor compared to those found in electrothermal and flame AAS, the multi-element capabilities of the system still make the system analytically viable. The future of CFSS in analytical chemistry lies in the application to a simultaneous multi-element furnace system. The furnace has the advantage of handling small sample sizes

and providing low absolute detection limits. Continuum source CFSS has the advantages of being a background corrected technique, a multi-element technique, and excitation over the entire absorption profile (normal or anomalous splitting). In addition a well-designed continuum source CFSS system with an AC magnet and an echelle spectrometer could also be used for multielement Zeeman atomic spectrometry as well as for multielement CFSS. Thus with a further reduction in the LODs and increased Useful Analytical Ranges (UARs), continuum source CFSS may become a viable analytical technique for multi-element analysis.

Davis and Winefordner (9) evaluated the noise characteristics of a multi-element Voigt-effect CFSS system. A fuel-rich air-acetylene flame was used as the atom reservoir in this study. A Glan-Foucault calcite prism polarizer, placed prior to the flame, was oriented at a 45° angle to the magnetic field. A second polarizer, the analyzer, was placed after the flame to detect the amount of light which is rotated. When the analyzer was oriented orthogonally to the first polarizer, the signal produced was proportional to the square of the concentration of the analyte. The CFSS signal could be linearized with respect to concentration by offsetting the analyzer by a small offset angle.

The study of the noise characteristics of the squared and the linear CFSS systems has helped to enumerate the various noise sources which will be encountered in both systems. The major source of noise for the squared system appeared to be shot noise from the flame and PM tube dark current, while the primary noise source for the linear system in this study was the flicker noise from the source used. Background spectra also demonstrated the CFSS effect for OH in the flame. Along with enumerating these problems, the results of this study have suggested various improvements which could be made in a Voigt effect CFSS system to optimize its performance in multi-element analysis. A

comparison of LODs for Ca 422.673 nm using Amplitude Modulation and DC measurement is given in Table 3.

Davis, et al. (10) have also evaluated a dye laser excited Voigt effect CFSS system. Our system employed a transverse magnetic field around either an air-acetylene flame or a graphite furnace. A second polarizer, the analyzer, was used to detect the amount of light which was rotated. Since the signal produced in CFSS was proportional to the incident intensity of light, it was postulated that the use of a laser as an excitation source for CFSS might be a useful technique. The results of our experiment showed the reverse to be true. Based on the limits of detection obtained (see Table 4), laser-excited CFSS did not appear to be a viable analytical technique. The results obtained, however, did provide interesting information in terms of the theoretical evaluation of CFSS.

TABLE 3

Limits of Detection in mg/L (S/N = 3) for Ca at 422.673 nm Using Amplitude Modulation (AM) vs DC Measurement

Polarizer Orientation	Measurement System	
	AM	DC
Squared System	0.2	0.2
Linear System	1.0	1.0

TABLE 4

Limits of Detection (μg/mL; S/N = 3) Obtained by Laser Excited CFSS

Element	λ(nm)	Detection Limit (μg/mL)	
		Flame	Furnace
Ca	422.67	0.3	--
In	303.94	1.0	--
Mg	285.21	0.1	--
Na	589.00	0.03	--
Pb	283.31	--	1.0
Sr	460.73	0.09	0.5

Atomic Fluorescence and Atomic Ionization in Flames and Furnaces. Rutledge, et al. (12) have evaluated several correction methods for several types of spectral and electrical interferences with a copper vapor pumped dye laser system are presented. A tunable pulsed dye laser pumped with a copper vapor laser was used to excite the atomic fluorescence of Li, Na, In, and Fe and the atomic ionization of Li, In, and Fe. Correction methods used involved either modulation of the pulsed laser output and subsequent subtraction of noise or electrical bandwidth limitation of the signals to enhance the signal to high frequency laser noise ratio. These methods provided a significant reduction in high frequency interference, a major noise source with this type of pump laser. These three correction methods were shown to provide a significant improvement in the detection power of both laser-enhanced ionization and fluorescence methods. Limits of detection (see Table 5) were presented for each correction method.

Two wavelength laser excited fluorescence and laser-enhanced ionization were investigated by Rutledge, et al. (13) for spatial profiling applications. A recently introduced absorption technique (which involved measuring the dif-

ferential absorption of a probe beam with a pump beam on and off) was also investigated for spatial profiling applications and determination of absolute number densities. This method, called concentration modulated absorption, was inferior to the fluorescence and ionization methods. A high-repetition rate, high average power copper vapor laser with a computer controlled data acquisition and beam scanning system was used for speed, repeatability and ease of data collection (see Figure 1). Design, construction, and associated operating parameters were discussed.

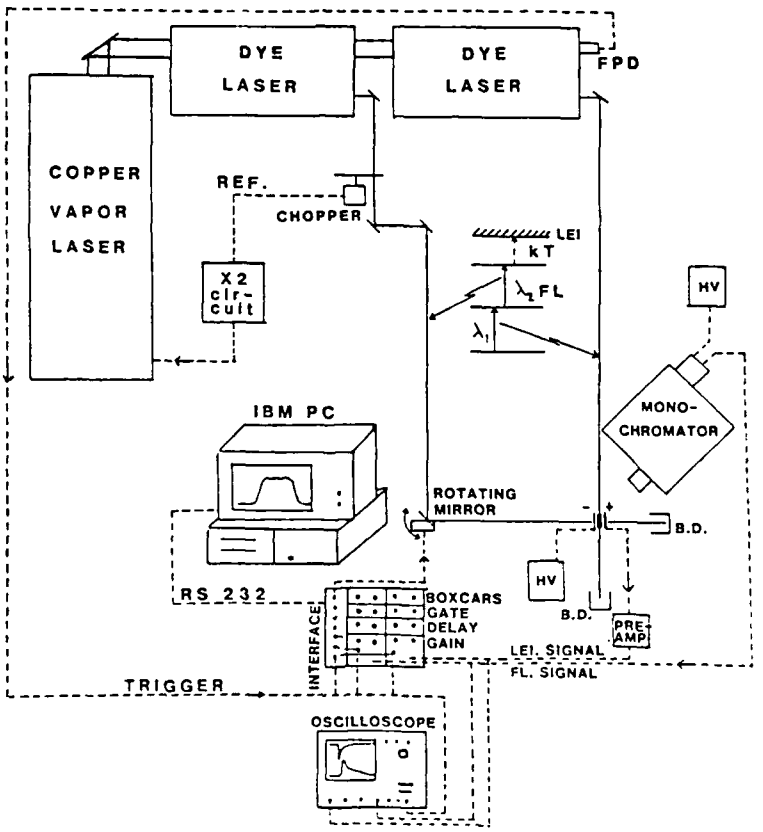

Fig. 1. Experimental Setup for Two Wavelength LEIS and LEAFS.

The two-wavelength LEIS and LEAFS results demonstrated exceptional spatial resolution and excellent sensitivity. The spatial results shown represented the first application of two-wavelengths LEIS and LAFS to this area. The high-repetitive rate laser used and an optical method of scanning the beams through the flame were shown to allow rapid determination of spatial profiles of analyte concentrations. While the applications here were limited in scope, it was felt that these techniques will find many applications.

Goforth and Winefordner (14,15) have described two unique graphite furnaces for use with laser excited atomic fluorescence. Laser excited atomic fluorescence in a graphite furnace gives detection limits (see Table 6) for Pb, Cu, Mn, Sn, Al, In, Li, and Pt, in the picogram to sub-picogram range (14). The linear dynamic range for these elements varies from 3 to 7 orders of magnitude. A graphite rod, a plain graphite cup, and a slotted graphite cup are compared as the cuvette in the fluorescence system. Detection limits for a pyrolytic coating, a tantalum foil liner, and a tantalum carbide coating of the graphite cuvette are compared. A hydrogen-argon atmosphere, a low pressure atmosphere, and an argon atmosphere are compared as the atmosphere surrounding the graphite cuvette. Lastly, Cu and Mn are determined in several Standard Reference Materials.

TABLE 5

Limits of Detection (ng/mL), for All Measurement Methods

Copper Vapor Dye Laser

	CONV	ABS	BLIA	$\lambda_{ex}/\lambda_{em}$ nm
Laser-Enhanced Ionization Detection				
Li	2	0.3	0.1	670.8
Fe	30	5.0	2.0	296.7
In	4	0.6	0.2	303.9
Laser-Enhanced Fluorescence				
Li	14	0.8	0.4	670.8/670.8
Fe	98	18.0	5.0	296.7/373.5
In	43	8.0	2.0	303.9/325.9
Na	14	3.0	1.0	589.0/589.0

Excimer Dye Laser

Laser-Enhanced Ionization Detection				
Li	0.7	0.3	0.5	670.8
Na	4.0	1.0	2.0	296.7
In	0.2	0.2	0.4	303.9

Copper Vapor Dye Laser

Bandwidth Limited Signal Processing (BLSP) - Fluorescence Detection		
Li	2	670.8/670.8
Fe	15	296.7/373.5
In	3	303.9/325.9
Na	2	589.0/589.0

CONV - Conventional method of measuring pulsed laser signals using a boxcar averager and gated integrator.

ABS - Active baseline subtraction method using a modulated pulsed laser. Subtraction of background noise is done by the boxcar special electronics.

BLIA - Boxcar averager plus lock-in amplifier using a modulated pulsed laser. Subtraction of background noise is accomplished in the lock-in amplifier.

Footnotes To Table 5 - Continued

BLSP - Bandwidth limited signal processing in which high frequency laser noise is not amplified while the signal is amplified to increase signal to noise ratio of fluorescence signals.

TABLE 6

Comparison of Hydrogen-Argon (H_2-Ar), Argon (Ar), and Low Pressure (LP) Atmospheres[a]

	Limits of Detection (pg)[b]			UAR[c]			Slope[d]		
	H_2-Ar	Ar	LP	H_2-Ar	Ar	LP	H_2-Ar	Ar	LP
Cu	$7.x10^{0}$	$2.x10^{0}$	$2.x10^{2}$	4.5	5	3	0.91	1.05	0.95
Mn	$7.x10^{0}$	$1.x10^{0}$	$7.x10^{0}$	3	4	3	0.98	0.98	1.05
Pt	$6.x10^{1}$	$1.x10^{0}$	$2.x10^{1}$	3	3.5	>5	0.93	1.05	0.90
Sn	$2.x10^{-1}$	$1.x10^{1}$	--	>6	5	-	1.00	0.95	--
In	$5.x10^{-2}$	$3.x10^{-1}$	$7.x10^{-1}$	6	6	5	1.10	0.91	1.50
Li	$4.x10^{2}$	$4.x10^{2}$	$4.x10^{3}$	3	3	2.5	0.90	0.92	0.62

[a] 5 µL aliquots

[b] Limit of detection is defined as 3 σ/m, where σ = standard deviation of the blank and m = slope of calibration of curve.

[c] Useful Analytical Range (orders of magnitude).

[d] Slope of log signal vs log mass calibration curve.

Goleorth and Winefordner (15) also designed a unique furnace-laser excited fluorescence system in which the laser excitation and the fluorescence collection optics are co-linear to allow use of the conventional AA furnace systems. Detection limits are given in Table 7. The instrumental system is shown in Figure 2.

TABLE 7

Limits of Detection by Laser Atomic Fluorescence Spectroscopy[a] for the Tube Furnace

	Wavelength, (nm)		Limits of Detection (pg)		
Element	Exc	FL	Tube[b]	Cup[c]	GFASS[d]
Al	394.4	396.2	$1x10^2$	$5.x10^{2c}$	$1.x10^0$
Cu	324.8	327.4	$8.x10^0$	$2.x10^0$	$2.x10^0$
Mo	313.3	317.0	$1.x10^2$	NS[f]	$1.x10^2$
V	385.6	411.2	$2.x10^5$	NS[f]	$2.x10^1$

[a]Limit of detection is defined as $3\sigma/S$, where σ = standard deviation of the blank and S = slope of calibration curve; 5 µL volumes were used.

[b]This work.

[c]Previous work from this laboratory, (7).

[d]From other works.

[e]Hydrogen-argon atmosphere.

[f]No signal.

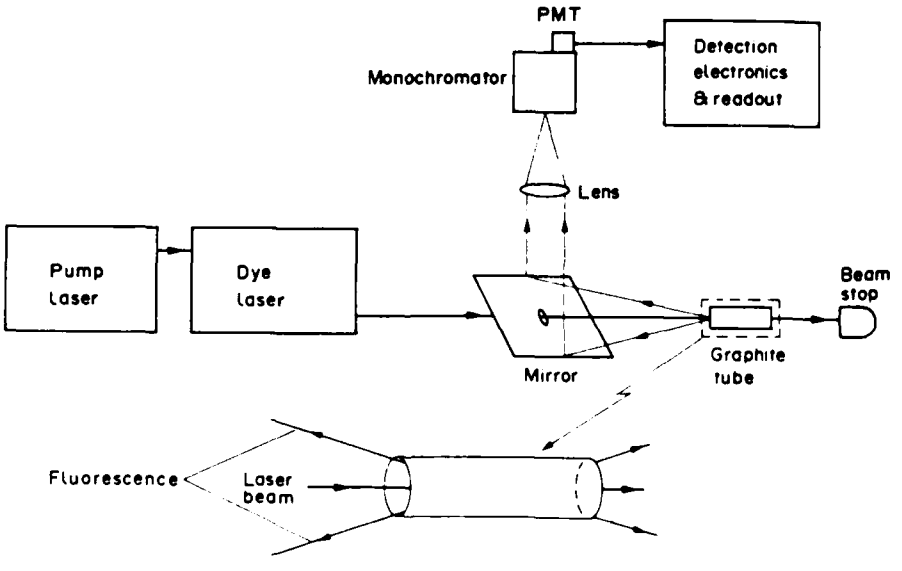

Fig. 2. Optical Arrangement of Tube Furnace System for Laser-Excited Atomic-Fluorescence

Patel and Winefordner (16) have used a demountable glow discharge source for the atomization of the analyte solutions deposited on graphite and copper rod cathodes. Indium atoms were sputtered-atomized from the cathode surface and excited by a pulsed, frequency-doubled dye laser pumped by the nitrogen laser. Atomic fluorescence measurements were performed using a non-resonance fluorescence transition. The detection limits of indium in aqueous solutions (10 µL) deposited on graphite and copper electrodes were 8×10^{-9} and 11×10^{-9} g, respectively (8 ng and 11 ng).

Diagnostical Studies of the ICP. Krupa and Winefordner (17) have evaluated the RF power dependency of several elements employing ICP-AES and ICP-excited-ICP AFS and AAS in the extended sleeve torch. The fluorescence intensity of the non-refractory elements was shown to be inversely proportional to power, while the sensitivity for refractory elements increased with increasing rf power to the atomization cell ICP. The alkaline earth elements, however, have more than one maximum in the fluorescence vs power curves, which may be due to a complex equilibrium between these elements and the dissociation products of water. The influence of power and water vapor on the Ar metastable absorbance have also been investigated.

Although these results were inconclusive, they seemed to indicate that water and its dissociation products play a major role in the atomization/excitation process in the extended sleeve torch ICP. This was especially apparent for the Ar metastable population and might be responsible for the behavior of the alkaline earth metals. Work is presently in progress to determine spatially resolved populations in hydroxyl, hydrogen and oxygen species in the ICP. These measurements may provide us with information which will lead to an explanation of these curves, and to a better understanding of the extended sleeve torch atom reservoir.

Huang, et al. (18) have also studied the effect of RF power for the extended-sleeve torch ICP on laser excited fluorescence and emission. Relative laser excited fluorescence and emission intensities as a function of RF power were measured for Ca(I), Ca(II), Ba(I), Ba(II), Mg(I), Mg(II), Na(I) and Cu(I). The behavior of the signals as a function of RF power was found to show, in most cases, unexpected behavior compared to previous studies with a conventional short ICP torch. In some cases, unexpected dual maxima or minima occurred in such plots. The effect of an easily ionized element, K, on Ca(I) and Ca(II) fluorescence was also studied using the extended-sleeve torch and the results indicated a considerably larger ionization interference than exists with the conventional short torch. Although the extended torch has found some use for laser excited-ICP-fluorescence and ICP excited-ICP fluorescence, researchers should be wary of unexpected variations with power and substantial ionization interferences.

Huang, et al. (19) measured the radial distribution profiles of ground state atoms and/or ions for calcium, manganese, and copper in an inductively coupled plasma have been measured using an excimer (XeCl) pumped dye laser as an excitation source of fluorescence. As a comparison, radial emission profiles also have been measured with an Abel-inversion procedure. In our low-flow nebulizer plasma system at low observation heights, the profiles of excited state atoms and ions resembled each other with a minimum in the center of the plasma. The profiles of ground state atoms and ions, however, possessed a bell shape except for calcium ground state ions which had a doubled-peaked distribution.

Omenetto, et al. (20) showed that when two pulsed dye lasers are turned in spatial and temporal coincidence to two connected atomic transitions in a flame or plasma, the resonance fluorescence monitored from the first excited

level decreased due to the depletion of the population of that level induced by the second laser excitation step. The monitoring of such a decrease (fluorescence dip) was shown from simple theoretical considerations to be useful for diagnostic studies and for the evaluation of some fundamental parameters of the atomic transition involved in the second-excitation step. Both steady state and transient behaviour were discussed. The information content of the fluorescence dip was similar to that of the saturated fluorescence signal. However, several distinct advantages were offered by the new technique especially when the level reached by the second excitation step was close to the ionization limit of the atom.

Fluorescence dip spectroscopy is another tool for diagnostic studies of flames and plasma. From the theoretical considerations, the main characteristics features of the technique can be summarized as follows.

(1) When steady state conditions are warranted, as for example in the double-resonance ionic fluorescence case, the information provided by the fluorescence dip is the same as that obtainable by measuring the fluorescence from the final excited level under saturated conditions. The technique offers high spatial resolution since it probes the intersection of the two focussed laser beams. As in conventional fluorescence, scattering has to be avoided. However, the relative fluorescence dip is independent of the total number of atoms and therefore pre-filter and post-filter effects on the observed signal are unimportant.

(2) In the presence of ionization losses and metastable levels acting as traps for the atoms, time resolved fluorescence measurements of the dip are directly related to the absorption oscillator strength of the transition causing the dip. This feature is highly attractive, particularly when the second step is a two-photon absorption transition to a highly excited level

whose cross section can therefore be accurately evaluated. Here, the dip technique is significantly advantageous since the fluorescence from the final level would be hard to detect because of the ionization losses and the ionization signal is not unequivocally related to the absorption strength of the transition.

(3) In some cases, the first and second excitation transitions do not share a common level, i.e., when the upper level reached by the first step differs from the lower level of the second excitation step. This would occur when the first laser couples levels 1 and 2 while the second laser connects levels 2' and 3. In this case, a dip in the resonance fluorescence signal may or may not be observed, depending upon the character of level 2', i.e., on how fast this level is coupled with level 2. If level 2' is metastable, a dip should not be observed during the short interaction time considered in this paper. On the other hand, if levels 2' and 2 are strongly coupled by collisions, a dip should easily be observed. It then follows that fluorescence dip spectroscopy can also be used to study relaxation effects between levels.

(4) When the second excitation step proceeds directly into the ionization continuum (photoionization) or reaches a Rydberg level from which collisionally assisted ionization is almost instantaneous, the absolute magnitude of the fluorescence dip will reflect the ionization yield.

Li, et al. (21) have calculated and measured axial signal profiles of analyte molecular, atomic, and ionic excitation. Such profiles are easier to deal with theoretically than radial profiles because the central channel is more homogeneous than any other part of the part in the plasma.

The large radial regions investigated in spatially resolved measurements may render the conventional LTE-based models inappropriate for mechanism elucidation. A more general (stochastic) dynamic model was established, where

equilibria and steady states were considered as special cases. Kinetics of rate determining reactions such as dissociation, atomization, ionization, and recombination were considered. For mathematical simplification, we imagined that the vapor plume resulted from a single aerosol particle and the kinetic processes taking place were then closely followed. In our case, diffusion was approximated as volume expansion under constant pressure. The resultant analyte distribution observed should then be a good approximation to the real one, assuming an ICAP with reproducible experimental conditions and a uniform solution droplet size distribution. By comparison of the simulated height profiles using different rate constants with experimental height profiles, analyte atomization and ionization could be more precisely described. On the other hand, measurements of experimental height and evaluation of statistical moments allows estimation of reaction rate constants.

Li, et al. (22) also have measured the height-resolved atomic and ionic emission profiles of calcium and magnesium were characterized by their statistical moments. The zeroth and first moments were employed for estimating rate constants of atomization, k_D, ionization, k_I, recombination, k_R, and vapor plume expansion, k_X. Because the initial number density, n_o, of the molecular analyte species in the vapor plume resulting from a single solution droplet was not measurable, only k_I could be estimated directly from the signal profiles. Rate constants k_D and k_R could be calculated using an educated guess of k_X. The expansion constant, k_X, could only vary within a narrow range limited by the difference $w = (S_1)_i - 1/\beta$, i.e,. $1/w<k_X<2/w$, where $S_1)_i$ represents the 1st moment of species i and β was the sum of rate constants $k_F + k_R + k_X$. Comparison of signal and simulated profiles the rf power dependence of k_X. As rf power was increased, k_X decreased slightly, resulting in a significant increase in k_D.

The power dependencies of k_I for Ca was different from that for Mg. The fast increase in k_I with rf power made ionization less favorable as a rate determining step in Ca excitation at high power. Mg had a k_I nearly independent of rf power. Its atomic and ionic profiles varied with power in the same manner, whereas Ca(I) profiles showed a shift with power. Furthermore, Mg(II)/Mg(I) ratio at a given height was essentially invariant with solution concentration.

Surface Burners for Atomic Spectrometry. Krupa, et al. (23-25) have designed surface burners for diffusion flames for use in atomic absorption, emission, fluorescence, and ionization spectrometry. These burners produced extremely laminar, homogeneous flames which did not flashback even for such high burning velocity gas mixtures as C_2H_2/O_2 H_2/O_2, etc. These burners will be of use in combustion diagnostics (25) as well as analytical chemistry (23,24). Several flame types with measured temperatures are given in Table 7.

Because of the versatility of such burners, flames with almost any temperature and composition can be prepared with no danger of flashbacks. The addition of oxygen to a premixed air-C_2H_2 flame improved AA LODs for some elements, particularly Ca and Cr, by an order of magnitude or more. However, the LODs of refractory elements were 1-2 orders of magnitude worse than in the premixed N_2O-C_2H_2 flame, even though temperatures up to 3000 K were achieved with the oxyhydrogen diffusion flame (see Table 8); these LODs should be improved by switching to a N_2O-C_2H_2 primary flame with the addition of O_2 at the surface.

The diffusion flames which were produced on this burner were immune to flashbacks. Because of this, any slot width could be tolerated. Making the slot wider would provide a suitable burner for the nebulization of slurry samples which could readily clog conventional slot burners.

TABLE 8

Measured Flame Temperature of Various Fuels Burning in Oxygen and Diluted with Argon

Fuel	Temperature Range (K)
H_2	1190-3160
CH_2	2360-2990
C_2H_2	2140-3470
Gasoline	2230-2750
Hexane	2590-2910

Other Diagnostical Studies. Zizak, et al. (26) reported the first use of a cross beam polarization spectrometry method with pulsed dye lasers in flames. In this work, polarization spectroscopy has been used in a flame with a beam-crossing configuration. The potential utility of the technique for combustion diagnosis has been investigated. A probe volume of <1 mm^3 could be easily achieved with a low crossing angle between the beams, and single-shot signals could be detected in atmospheric pressure acetylene-air flame. Use of a pulsed dye laser offered the possibility of extending the technique to other atomic or molecular species, which absorb in the visible or UV spectral regions. The rather low sensitivity obtained in our experiments could be improved by an order of magnitude or more by use of a better experimental arrangement (e.g., better polarizers). The major drawback of the polarization technique for combustion diagnotics seemed to be due to the collisional redistribution of the population of the magnetic sublevels. The influence of gas composition on the signal strength must be investigated for quantitative measurements of total number densities in the combustion gases.

Patel and Winefordner (27) have evaluated a demountable glow discharge

source as an atomization source (cell) for atomic spectrometric studies of several analytes sputtered from copper and graphite cathodes. The constituents of sample material (major, minor and trace levels) atomized in the glow discharge source during the sputtering process have been studied from the characteristic emission spectra of the excited species. Atomic, ionic, and molecular species have been observed depending upon the experimental conditions in the source. The performance of the di harge source with respect to the influence of various parameters on intensities and intensity ration - current, voltage, pressure, and type of support gas - on spectral characteristics have been investigated in order to optimize conditions leading to the highest number densities of the analyte species, the lowest spectral backgrounds, and minimal interferences. Spectroscopic excitation temperatures and electron number densities have also been evaluated.

Zizak, et al. (28) have developed a cross-beam saturated interference spectroscopic method for spatial number density profiles in flames and plasmas. The technique involved the use of a pulsed N_2-dye laser producing 2 counterpropagating probe beams which underwent constructive interference at the detector. A pump beam which interacted with analyte species in one of the beams destroyed the zero base line resulting in a signal proportional to the square of the number density. Unfortunately, the method was subject to spatial and temporal difficulties of the probe beam resulting in a poor signal-to-noise ratio and had a poor sensitivity.

Other Analytical Studies. Kujirai, et al. (29) designed and evaluated a second derivative, wavelength modulated atomic emission-atomic fluorescence flame spectrometer. Atomic emission and fluorescence signals were collected simultaneously with sinusoidal wavelength modulation and detection of the second harmonic mode. The system consisted of a continuum source, a mono-

separated air/acetylene flame and a wavelength-modulated monochromator. Limits of detection of several elements were measured. This method was applied to the analysis of a copper alloy, and Co, Cu, Fe, Mn, Ni, Pb, and Zn were successfully determined.

Lanauze and Winefordner (30) evaluated the use of pulsed laser photoacoustic flame spectrometry for elemental analysis. This approach has been applied for the first time as a technique for elemental analysis in flames. The limit of detection achieved for Na was 780 ng/mL. For Mn, Sr, Tl, and Ca, the sensitivity was found to be very poor as compared with Na, but no explanation is available at the moment. Photoacoustic spectroscopy is not expected to be as sensitive as any of the now existing spectroscopic techniques for elemental analysis.

Modification on the system used (30) could lead to an enhancement of the signal to noise. Minimization of the flame background acoustic noise, a higher laser irradiance so as to achieve saturation of the transition, use of a signal averager to acquire and integrate the complete waveform, and correlation techniques are some of the possible improvements. Despite this, photoacoustic spectroscopy is not expected to be more sensitive than emission, absorption or fluorescence spectroscopy. Also, in contrast to the optical methods mentioned, simultaneous multielement analysis is not possible with photoacoustic spectroscopy or with any other photothermal method since selectivity is achieved only in the excitation step. Even in the area of combustion diagnostics, the technique is not expected to have much impact because of the difficulty of obtaining spatially resolved measurements and the apparent impossibility of applying the technique to real (turbulent) combustion systems.

Lanauze and Winefordner (31) also applied pulsed dye laser polarization spectroscopy to elemental analysis in flames. The approach involved the detection of a coherent beam of light (dye light), and so the detector could be situated far away from the sampled point (120 cm in our case). In this way, the solid angle defined by the detector could be made very small, and the contribution to the background from fluorescence, scatter, and/or emission become negligible. By the nebulization of 1000 mg/L solutions of Na and Al (as $AlCl_3$) into the flame to check for fluorescence and scatter in the presence of the pump beam (no probe beam), no measurable change in the background could be observed. The limit of detection for Na (S/N = 3) was found to be 2 µg/L for averaging 3000 pulses. It must be pointed out that this limit of detection was obtained with a maximum achievable extinction ratio of only 200. Assuming shot-noise-limited conditions, and improvement in the polarizer extinction ratio of 10^4 (an extinction ratio of 10^6 is specified for these polarizers) would decrease the limit of detection to ~20 ng/L (i.e., 20 pptr). Further reduction in the extinction ratio, better beam quality, detector with a higher sensitivity and lower dark current when working near the limit of detection, higher pump intensity (only ~500 µJ/pulse was available from our system), and use of fine-adjustment rotators for the polarizers should result in further improvement of limits of detection. Based on these preliminary results, we expect polarization spectroscopy to become a very sensitive technique for trace elemental analysis.

Other Analytical Studies. Tremblay, et al. (32) studied the direct introduction of solid samples into an inductively coupled plasma (ICP) was studied using ablation of metals by a focused XeCl excimer laser. The laser pulses formed a very energetic microplasma at the metal surface from which the

ablated species were carried into a stream of argon and were detected using a gated integrator/boxcar averager. This method was applied to the analysis of Ni and Cr in stainless steel.

Tremblay, et al. (33) also used a pulsed tunable dye laser pumped with an excimer laser to excite ionic fluorescence of the rare earth elements in the inductively coupled plasma. Because several fluorescence lines have been observed after laser excitation, it was possible to draw partial energy level diagrams for most of the rare earths. Non-resonance fluorescence lines were used for all measurements in order to minimize spectral interferences. Detection limits at given excitation wavelengths are reported for each element (see Table 9). Laser excited ionic fluorescence has eliminated the problem of spectral interferences which has been associated with the analysis of the rare earths by atomic emission spectrometry in the inductively coupled plasma.

Yeah, et al. (34) evaluated the hollow cathode lamp-inductively coupled plasma-atomic fluorescence spectrometer system (Baird) for the measurement of Na, Cu, Ni, Ag, Fe, Al, Cr, and Mg in a variety of organic solvents. Kerosene proved to be the best solvent. The system was evaluated for the effect of solution flow rate, oil content, O_2 flow rate, RF power and observation height for the measurement of those eight elements in a 2% oil-98% kerosene mixture. Analytical figures of merit, including detection limits (see Table 10), linear ranges of response, stability with time, and spectral interferences, were evaluated for the 8 elements present as metallorganic compounds. The analysis of several standard reference materials showed excellent agreement with the certified values.

TABLE 9

Fluorescence Transitions and Detection Limits for the Rare Earth Elements in the Inductively Coupled Plasma

Rare Earth Element	Excitation Wavelength (Transition, cm^{-1})[a] $\ell \rightarrow u$	Fluorescence Wavelength (nm) (Transition, cm^{-1})[a] $\ell \rightarrow u$	Fluorescence Process[b]	Detection Limit (ng/mL)	Detection Limit By ICP-ES (ng/ml)[c]
La	403.169 (2592 - 27388)	379.083 (1016 - 27388)	AS-DLF	170.	10.
Dy	407.798 (828 - 25343)	394.470 (0 - 25343)	AS-DLF	400.	10.
Gd	407.844 (4841 - 29353)	354.580 (1159 - 29353)	AS-DLF	75.	14.
Ce	407.585 (4911 - 29439)	401.239 (4523 - 29439)	AS-DLF	400.	48.
Er	404.835 (7150 - 31844)	374.265 (5133 - 31844)	AS-DLF	260.	10.
Nd	406.109 (3802 - 28419)	428.452 (5086 - 28419)	S-DLF	470.	50.
Pr	406.134 (5108 - 29724)	405.654 (5079 - 29724)	AS-DLF	240.	37.
Tb[d]	403.306 (?)	400.557 (?)	?	650.	23.
Lu	302.054 (12435 - 45532)	296.332 (11796 - 45532)	AS-DLF	85.	1.0
Tm	301.530 (237 - 33392)	313.136 (0 - 31927)	S-SWF	140.	5.2
Yb	303.111 (0 - 32982)	297.056 (0 - 33654)	AS-SWF	25.	1.8
Eu	305.494 (1669 - 34394)	290.668 (0 - 34394)	AS-DLF	72.	2.7

[a]Energy levels in cm^{-1}; l = lower level; u = upper level

[b]AS-SWF = Stokes-Stepwise Fluorescence; AS-SWF = Antistokes-Stepwise Fluorescence; S-DLF = Stokes-Direct Line Fluorescence; and AS-DLF = Antistokes-Direct Line Fluorescence

[c]Detection limits were from reference 6

[d]Energy levels were not identified for Tb.

TABLE 10

Analytical Figures of Merit for Several Metals in Organic Solvents by HCL-ICP-AFS[a]

	Analytical Figures of Merit (µg/mL)	
Metal	Detection Limit[b]	Upper Concentration[c]
Na	0.006	10
Cu	0.05	250
Al	0.1	500
Cr	0.1	250
Fe	0.01	500
Ni	0.07	500
Ag	0.03	125
Mg	0.0004	10

[a]RF power = 500 W; 1.0 mL/min solution introduction rate; 30 cm^3/min O_2 flow rate

[b]Detection limit defined as concentration giving S/N = 3

[c]Upper concentration is that concentration where the calibration curve has decreased to 5% of the value on the linear curve

REFERENCES (All supported by AFOSR)

1. N. Omenetto and J.D. Winefordner, "Atomic Fluorescence Spectrometry the Inductively Coupled Plasma," Chapter 9 in Inductively Coupled Plasmas In Analytical Atomic Spectroscopy, A. Montaser and D.W. Golightly, editors, Plenum Press, in press.

2. N. Omenetto and J.D. Winefordner, Prog. Anal. Atom. Spectrosc., 8, 371 (1985).

3. T. Hasegawa and J.D. Winefordner, Spectrochim. Acta, 42B, 773 (1987).

4. T. Hasegawa and J.D. Winefordner, Spectrochim. Acta, 42B, 651 (1987).

5. T. Hasegawa and J.D. Winefordner, Spectrochim. Acta, 42B, 637 (1987).

6. G. Zizak, J. Lanauze, and J.D. Winefordner, Comb. and Flame, 65, 203 (1986).

7. B.W. Smith, M.J. Rutledge, and J.D. Winefordner, Appl. Spectrosc., 41, 613 (1987).

8. M.J. Rutledge, B.W. Smith, J.D. Winefordner, and N. Omenetto, Anal. Chem., 59, 1794 (1987).

9. L.A. Davis and J.D. Winefordner, Anal. Chem., 59, 309 (1987).

10. L.A. Davis and J.D. Winefordner, Spectrochim. Acta, 41B, 1167 (1986).

11. L.A. Davis, R.J. Krupa, and J.D. Winefordner, Spectrochim. Acta, 42B, 669 (1987).

12. M.J. Rutledge, M.E. Tremblay, and J.D. Winefordner, Appl. Spectrosc., 41, 5 (1987).

13. M.J. Rutledge, M. Mawn, B.W. Smith, and J.D. Winefordner, Appl. Spectrosc., submitted.

14. D. Goforth and J.D. Winefordner, Talanta, 34, 290 (1987).

15. D. Goforth and J.D. Winefordner, Anal. Chem., 58, 2598 (1986).

16. B.M. Patel and J.D. Winefordner, Spectrochim. Acta, 41B, 469 (1986).

17. R.J. Krupa and J.D. Winefordner, Spectrochim. Acta, 41B, 1015 (1986).

18. X. Huang, D. Mo, K.S. Yeung, and J.D. Winefordner, Anal. Chim. Acta, 184, 299 (1986).

19. X. Huang, K.S. Yeung, and J.D. Winefordner, Spectrochim. Acta, 40B, 1379 (1985).

20. N. Omenetto, G.C. Turk, M. Rutledge, and J.D. Winefordner, Spectrochim. Acta, 42B, 607 (1987).

21. K.P. Li, M. Dowling, T. Fogg, T. Yu, K.S. Yeah, J.D. Hwang, and J.D. Winefordner, Anal. Chem., submitted.

22. K.P. Li, T. Yu, J.D. Hwang, K.S. Yeah, and J.D. Winefordner, Anal. Chem., submitted.

23. R.J. Krupa, L.A. Davis, T.F. Culbreth, B.W. Smith, and J.D. Winefordner, Anal. Chem., 58, 3263 (1986).

24. R.J. Krupa, T.F. Culbreth, B.W. Smith, and J.D. Winefordner, Appl. Spectrosc., in press.

25. R.J. Krupa, G. Zizak, and J.D. Winefordner, Appl. Optics, 25, 3600 (1986).

26. G. Zizak, J. Lanauze, and J.D. Winefordner, Appl. Optics, 25, 3242 (1986).

27. B.M. Patel and J.D. Winefordner, Canad. J. Spectrosc., submitted.

28. G. Zizak, J. Lanauze, and J.D. Winefordner, Appl. Optics, 24, 3319 (1985).

29. O. Kujirai, L.A. Davis, and J.D. Winefordner, Spectrosc. Lett., 18, 781 (1985).

30. J.A. Lanauze and J.D. Winefordner, Spectrochim. Acta, 41B, 407 (1986).

31. J.A. Lanauze and J.D. Winefordner, Appl. Spectrosc., 40, 709 (1986).

32. M.E. Tremblay, B.W. Smith, M.B. Leong, and J.D. Winefordner, Spectrosc. Lett., 20, 311 (1987).

33. M.E. Tremblay, B.W. Smith, and J.D. Winefordner, Anal. Chim. Acta, in press.

34. K.S. Yeah, W. Masamba, and J.D. Winefordner, Anal. Sciences, in press.

END

FEB.

1988

DTIC